Structure
Article

Structure of RapA, a Swi2/Snf2 Protein that Recycles RNA Polymerase During Transcription

Gary Shaw,[1] Jianhua Gan,[1] Yan Ning Zhou,[1] Huijun Zhi,[1,3] Priadarsini Subburaman,[1] Rongguang Zhang,[2] Andrzej Joachimiak,[2] Ding Jun Jin,[1,*] and Xinhua Ji[1,*]
[1]Center for Cancer Research, National Cancer Institute, National Institutes of Health, Frederick, MD 21702, USA
[2]Structural Biology Center, Argonne National Laboratory, Argonne, IL 60439, USA
[3]Present address: Department of Microbiology and Immunology, Uniformed Services University of the Health Sciences, Bethesda, MD 20814, USA.
*Correspondence: djjin@helix.nih.gov (D.J.J.), jix@ncifcrf.gov (X.J.)
DOI 10.1016/j.str.2008.06.012

SUMMARY

RapA, as abundant as σ^{70} in the cell, is an RNA polymerase (RNAP)-associated Swi2/Snf2 protein with ATPase activity. It stimulates RNAP recycling during transcription. We report a structure of RapA that is also a full-length structure for the entire Swi2/Snf2 family. RapA contains seven domains, two of which exhibit novel protein folds. Our model of RapA in complex with ATP and double-stranded DNA (dsDNA) suggests that RapA may bind to and translocate on dsDNA. Our kinetic template-switching assay shows that RapA facilitates the release of sequestered RNAP from a posttranscrption/posttermination complex for transcription reinitiation. Our in vitro competition experiment indicates that RapA binds to core RNAP only but is readily displaceable by σ^{70}. RapA is likely another general transcription factor, the structure of which provides a framework for future studies of this bacterial Swi2/Snf2 protein and its important roles in RNAP recycling during transcription.

INTRODUCTION

Members of the Swi2/Snf2 family, classified into 25 subfamilies including a RapA group, mediate mobilization of various nucleic acid-protein complexes to facilitate gene expression (Flaus et al., 2006). A total of 1306 sequences have been identified for the 24 non-RapA subfamilies; they play important roles in many nuclear processes such as replication, transcription, DNA repair, and recombination (Brown et al., 2007; Dirscherl and Krebs, 2004; Flaus et al., 2006; Mohrmann and Verrijzer, 2005; Pazin and Kadonaga, 1997; Wu and Grunstein, 2000). So far, most of the studies on Swi2/Snf2 have focused on proteins that show transcriptional regulation mediated by ATP-dependent remodeling of chromatin structure (Dürr et al., 2006; Flaus et al., 2006; Pazin and Kadonaga, 1997; Tsukiyama and Wu, 1997). Although the mechanism of Swi2/Snf2 is largely unknown, crystal structures for the ATPase core of a Swi2/Snf2 protein, Rad54, revealed two helical Swi2/Snf2-specific domains that are fused to a RecA-like architecture found in the DExx box helicases (Dürr et al., 2005; Thomä et al., 2005).

RapA (also known as HepA) represents 220 bacterial/archaeal members in the RapA group, among which *Escherichia coli* RapA (Swiss-prot entry P60240) remains the only member for which a biological function has been demonstrated (Bork and Koonin, 1993; Eisen et al., 1995; Flaus et al., 2006; Kolsto et al., 1993; Lewis et al., 1992). It is an RNA polymerase (RNAP)-associated protein with ATPase activity; it also binds to DNA and RNA (McKinley and Sukhodolets, 2007; Muzzin et al., 1998; Sukhodolets and Jin, 1998). We showed previously that RNAP becomes sequestered or immobilized in a posttranscrption/posttermination complex (PTC) after one or few rounds of transcription, and that RapA reactivates the sequestered RNAP during multiround transcription in vitro (Sukhodolets et al., 2001). RapA-mediated RNAP recycling is dependent on the ATPase activity of RapA; the ATPase activity of RapA is stimulated upon the binding of RapA to RNAP (Sukhodolets et al., 2001; Sukhodolets and Jin, 2000). The mechanism whereby RapA reactivates the immobilized RNAP is unknown. We hypothesized previously that RapA can remodel the PTC and thereby reactivate the sequestered RNAP for transcription reinitiation (Sukhodolets et al., 2001).

In *E. coli*, RNAP exists in two forms, the core RNAP (CORE) and the RNAP holoenzyme (HOLO). The CORE, consisting of subunits $\alpha_2\beta\beta'$, is capable of transcription elongation and termination; whereas the HOLO, consisting of $\alpha_2\beta\beta'\sigma$, is capable of transcription initiation from promoters on a DNA template (Burgess et al., 1987; Travers and Burgess, 1969). We showed previously that RapA forms a complex with either the CORE or the HOLO, but with higher affinity for the CORE, suggesting that the RapA-binding site on RNAP may be distinct from the σ-binding site (Sukhodolets and Jin, 1998, 2000). Other works showed, however, that the protein binds to the CORE but not to the HOLO, suggesting that RapA and σ factor may share a common binding site (Muzzin et al., 1998). As the first step in our effort to establish the structure-and-function relationship of RapA, we determined the crystal structure of full-length *E. coli* RapA in complex with a sulfate ion (RapA•SO_4) at 3.2-Å resolution. Our data provide a framework for understanding RapA-dependent RNAP recycling as well as a guide for further studies aimed at dissecting the precise mechanism of bacterial transcriptional regulation in general and of RNAP recycling in particular.

RESULTS

Overall Structure

We determined the full-length structure of *E. coli* RapA via multiwavelength anomalous diffraction phasing at 3.2-Å resolution. Detailed statistics for phasing and refinement can be found in

Table 1. Data Collection, Phasing, and Refinement Statistics

	Full Length			
	Crystal 1		Crystal 2	Ntd
Data collection				
Wavelength (Å)	0.97935	0.97951	0.97935	0.97922
Resolution (Å)	50–3.4	50–3.4	50–3.2	30–2.15
Space group	$P4_32_12$	$P4_32_12$	$P4_3$	C2
Unit cell parameters (Å)				
a	123.8	123.7	123.9	219.5
b	123.8	123.7	123.9	39.2
c	187.7	187.5	188.0	61.3
R_{merge} (%)[a]	14.6	14.7	9.7	9.1
I/σ	24.1	22.3	11.9	9.7
Completeness (%)	99.9	99.9	97.3	90.4
Redundancy	17.0	17.0	3.8	3.1
Refinement				
No. of reflections			44,669 (2166)[d]	[e]
Nonhydrogen atoms				
Protein			15,332	
Sulfate ion			10	
R factor (%)[b]			25.0 (35.7)	
R_{free} (%)[c]			30.0 (43.4)	
B factor, Wilson plot ($Å^2$)			84.1	
B factor, overall ($Å^2$)			68.7	
RMSD				
Bond distances (Å)			0.016	
Bond angles (°)			1.5	
Ramachandran plot				
Most favored			64.5	
Disallowed			0	

[a] $R_{merge} = \Sigma|(I - < I >)| / \Sigma(I)$, where I is the observed intensity.
[b] R factor = $100 \times \Sigma| |Fo| - |Fc| | / \Sigma|Fo|$, where Fo and Fc are the observed and calculated structure factors, respectively.
[c] R_{free} was calculated with 5% of the data.
[d] Statistics in the highest resolution shell (3.20–3.31 Å) are shown in parentheses.
[e] The refinement of the Ntd structure is in progress, and the structure will be published elsewhere.

Table 1. There are two RapA•SO_4 complexes in the asymmetric unit, each containing 961 (residues 2-962) out of 968 amino acid residues and one sulfate ion. Among the 1922 amino acid residues, the backbone of seven and the side chains of 186 do not show perfect electron density (final 2Fo-Fc) at the contour level of 1.0 σ. Out of the 186 side chains, 112 are on the surface of the protein.

As depicted in Figure 1, the RapA structure contains seven domains and three linkers: an N-terminal domain (Ntd), two RecA-like domains 1A and 2A, two Swi2/Snf2-specific domains 1B and 2B, a Spacer domain, and a C-terminal domain (Ctd), and Linker1 between Ntd and 1A, Linker2 between 1B and 2B, and Linker3 between 2B and Spacer. Of the two crystallographically independent molecules, the backbones of their Linker1-to-Ctd fragments are virtually identical (root mean square deviation [RMSD] = 0.023 Å for 796 out of 855 pairs of Cα positions) and the backbones of their Ntd fragments are similar (RMSD = 0.318 Å for 105 out of 106 pairs of Cα positions). However, the relative positioning of the Ntd with respect to the Linker1-to-Ctd fragment is noticeably different in the two molecules (see Figure S1A available online) likely due to crystal packing.

The Ntd contains two subdomains, NtdA and NtdB, both folded as a highly bent antiparallel β sheet (Figure 1). This fold is also found in transcription factor NusG (Knowlton et al., 2003; Steiner et al., 2002), ribosomal protein L24 (Ban et al., 2000), human SMN (survival of motor neuron) protein (Selenko et al., 2001), mammalian DNA repair factor 53BP1, putative fission yeast DNA repair factor Crb2 (Botuyan et al., 2006), and bacterial transcription-repair coupling factor known as Mfd (Deaconescu et al., 2006). The functional roles of the Ntd homologs in these proteins suggest that the Ntd of RapA may interact with both nucleic acids and RNAP. The two RecA-like domains (1A and 2A) and the two Swi2/Snf2-specific domains (1B and 2B), containing a total of 514 amino acid residues, form the ATPase core of RapA, characteristic for the Swi2/Snf2 proteins (Figure 1). Both the Spacer and the Ctd are of the α/β fold in nature with a central β sheet flanked by helices and loops. The β sheet in the Spacer is antiparallel and flanked by three α helices, while the β sheet in the Ctd is mainly antiparallel and flanked by four α helices, among which the two longer helices exhibit a coiled-coil arrangement (Figure 1). Our structural comparison using the DALI server (Holm and Sander, 1996) indicates that the folds of both the Spacer and the Ctd are novel.

Figure 2 depicts the structural and sequence characteristics of RapA in detail. The three linkers contain 31, 25, and 44 amino acid residues, respectively. Linker1 is composed of three α helices, connecting the Ntd and the ATPase core; Linker2 consists of two β strands, tethering the two lobes of the ATPase core; and Linker3 contains three α helices, forming an elongated, L-shaped connector between the ATPase core and the Spacer. Representative electron density is shown for Linker3 in Figure 1. Together, Linker1 and Linker3 cover a distance of approximately 100 Å cross one face of the RapA molecule (Figures 1 and 2).

RecA-Like Architecture

RapA is capable of ATP hydrolysis (Muzzin et al., 1998; Sukhodolets and Jin, 1998). The structural basis for the ATPase activity is the RecA-like architecture formed by the two RecA-like domains 1A and 2A (Figure 3). Structure-based sequence alignment reveals the location of six functional motifs conserved for ATPase-core-containing proteins, including the DExx box helicases and members of the Swi2/Snf2 family (Figure 3).

The six functional motifs form two clusters: the cluster of motifs I-III is located in domain 1A and the cluster of motifs IV-VI is located in domain 2A (Figure 3E). As revealed by many helicase structures, motifs I (Walker A), II (Walker B or DExx box), III, V, and VI interact with MgATP while motifs III, IV, and V interact with nucleic acids (Caruthers and McKay, 2002). ADP or ATP analogs have been cocrystallized with many helicases such that the β-phosphate group of the nucleotide is bound in the P loop of motif I. In a zebra fish (Zf) Rad54•SO_4 structure (PDB entry 1Z3I), a sulfate ion is found in the P loop (Thomä et al., 2005). Similarly, a P loop-bound sulfate ion has been found in our RapA•SO_4 structure (Figures 1, 2A, and 3D). As demonstrated by mutational analysis, the six motifs are involved in chromatin remodeling

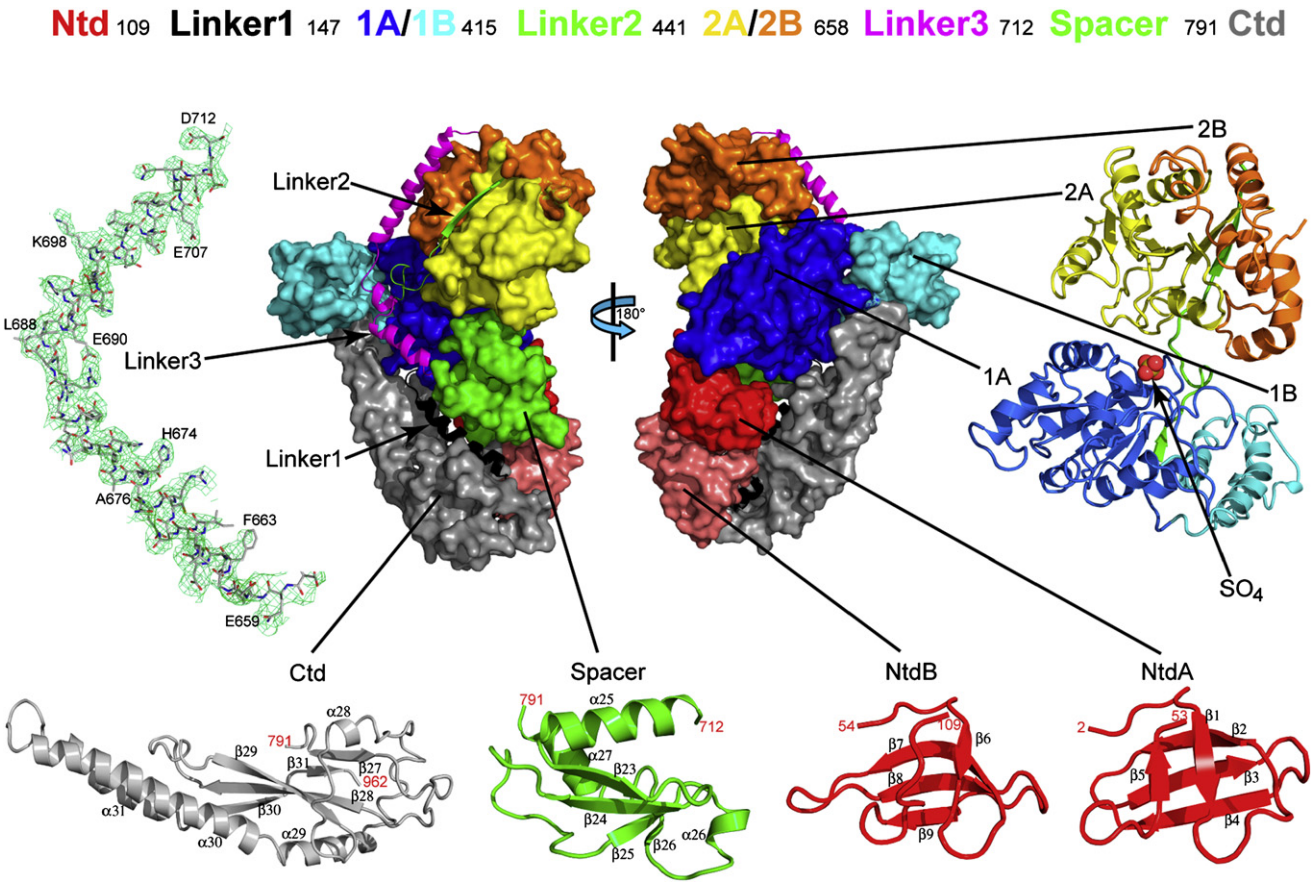

Figure 1. Overall Structure of *E. coli* RapA

On the top, the domain organization of RapA is shown with boundaries (residue numbers in the sequence). In the middle, the domain arrangement is shown schematically by two views of the molecule related to each other by a 180° rotation around the vertical axis. On the left, right, and bottom, the folds of individual domains and a cluster of four domains (1A, 1B, 2A, and 2B, which form the ATPase core of the enzyme) are illustrated. Both the orientation and the scale of the individual domains and the ATPase core are optimized for best viewing. The Ntd contains two sub-domains, NtdA and NtdB, which share the same fold. The Linker3 is illustrated as a stick model (C, gray; N, blue; O, red) outlined with the composite annealed omit map (green net, 2Fo - Fc, contoured at 1.0 σ). The Spacer and the Ctd exhibit novel folds. The sulfate ion bound to the ATPase core is shown as a sphere model. The color scheme used here (Ntd in red, Linker1 in black, 1A in blue, 1B in cyan, Linker2 in green, 2A in yellow, 2B in orange, Linker3 in magenta, Spacer in green and Ctd in gray) is also used in other figures.

and translocation on DNA (Dürr et al., 2005; Laurent et al., 1993; Thomä et al., 2005), and in RNAP recycling during transcription (Sukhodolets et al., 2001). Therefore, for the ATPase activity in general, and for the translocase activity in particular, the two clusters of functional motifs must be in close proximity to each other. As shown in Figure 3A, the two clusters in helicase PcrA face each other (Velankar et al., 1999). Similarly, the two clusters in the ZfRad54•SO_4 structure (PDB entry 1Z3I) also face each other (Figure 3B). This arrangement of the two RecA-like domains is apparently compatible with the ATP-hydrolysis activity. However, the two clusters in a *Sulfolobus solfataricus* (Ss) Rad54•DNA structure (PDB entry 1Z63, Figure 3C) are located on the opposite sides of the two RecA-like domains (Dürr et al., 2005). This arrangement of the two RecA-like domains, which was also observed in a ligand-free SsRad54 structure (PDB entry 1Z6A), was proposed to be the "open" conformation during translocation or DNA uptake (Dürr et al., 2005). Biochemical analysis of several SsRad54 mutants suggests that the RecA-like architecture of SsRad54 adopts a "closed" conformation that should be similar to that in ZfRad54•SO_4 (PDB entry 1Z3I, Figure 3B) for ATP hydrolysis. The "closed" (Figure 3B) and the "open" (Figure 3C) forms relate to each other by a dramatic 180° flip (Dürr et al., 2005).

The arrangement of the two RecA-like domains in our RapA•SO_4 structure (Figure 3D) is similar to those in PcrA•ATP•DNA (Figure 3A) and ZfRad54•SO4 (Figure 3B). This arrangement, compatible with ATP hydrolysis, is stabilized by additional domains that are present in RapA but absent from the Rad54 structures. Thus, the 180° flip of the 2A/2B lobe with respect to the 1A/1B lobe in the ATPase core of RapA may not occur during the functional cycle, although conformational changes are expected.

ATPase Core

The ATPase core of both RapA and Rad54 is composed of four domains, including 1A, 1B, 2A, and 2B (Figures 1 and 4). The two RecA-like domains 1A and 2A are conserved for many ATP-dependent nucleic-acid-manipulating enzymes. Domains 1B and 2B, on the other hand, are enzyme specific (Flaus et al., 2006).

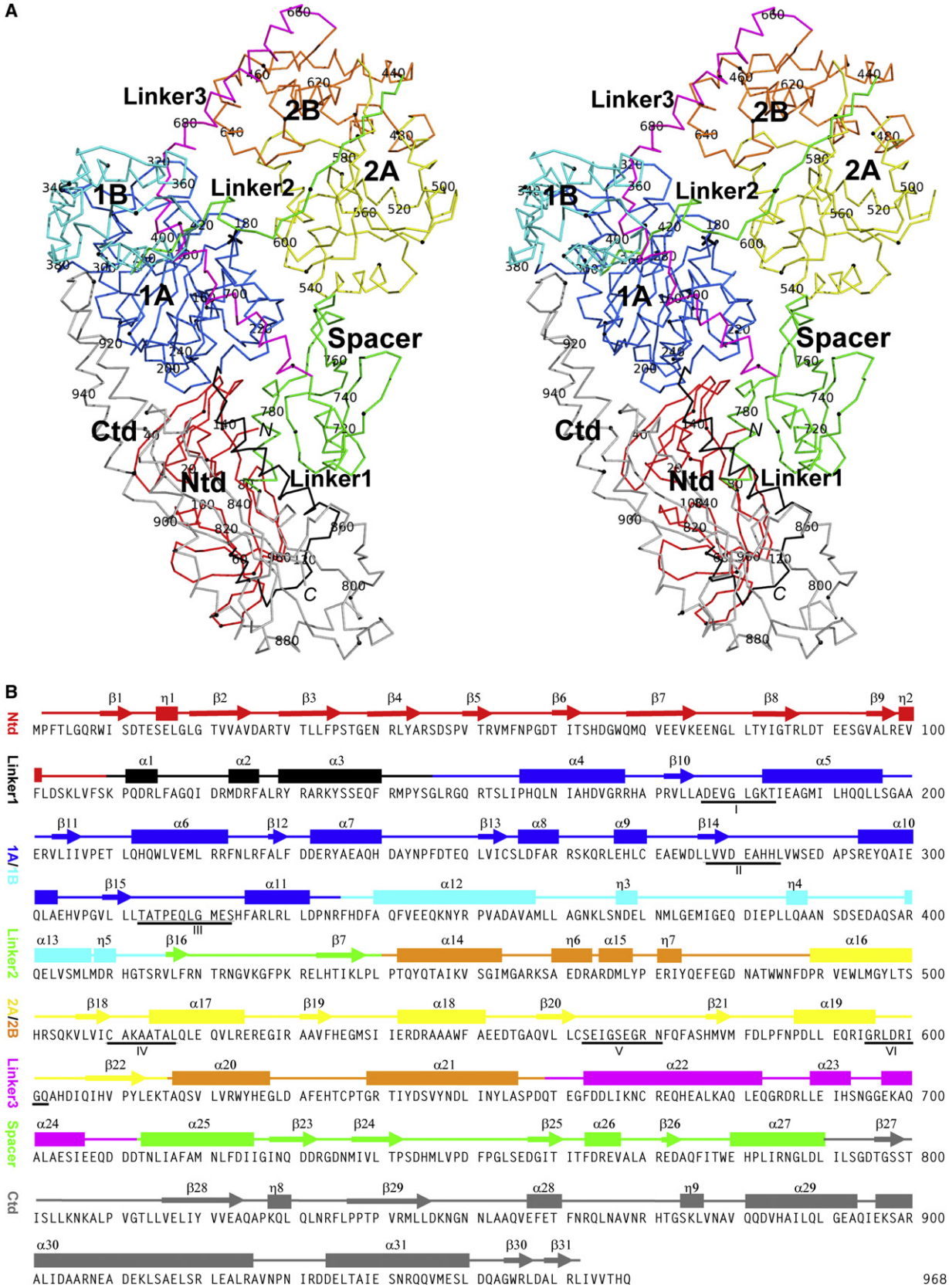
A
Linker3
2B
2A
1B
Linker2
1A
Spacer
Ctd
N
Ntd
Linker1
C
B
Ntd
Linker1
1A/1B
Linker2
2A/2B
Linker3
Spacer
Ctd
MPFTLGQRWI SDTESELGLG TVVAVDARTV TLLFPSTGEN RLYARSDSPV TRVMFNPGDT ITSHDGWQMQ VEEVKEENGL LTYIGTRLDT EESGVALREV 100
FLDSKLVFSK PQDRLFAGQI DRMDRFALRY RARKYSSEQF RMPYSGLRGQ RTSLIPHQLN IAHDVGRRHA PRVLLADEVG LGKTIEAGMI LHQQLLSGAA 200
ERVLIIVPET LQHQWLVEML RRFNLRFALF DDERYAEAQH DAYNPFDTEQ LVICSLDFAR RSKQRLEHLC EAEWDLLVVD EAHHLVWSED APSREYQAIE 300
QLAEHVPGVL LLTATPEQLG MESHFARLRL LDPNRFHDFA QFVEEQKNYR PVADAVAMLL AGNKLSNDEL NMLGEMIGEQ DIEPLLQAAN SDSEDAQSAR 400
QELVSMLMDR HGTSRVLFRN TRNGVKGFPK RELHTIKLPL PTQYQTAIKV SGIMGARKSA EDRARDMLYP ERIYQEFEGD NATWWNFDPR VEWLMGYLTS 500
HRSQKVLVIC AKAATALQLE QVLREREGIR AAVFHEGMSI IERDRAAAWF AEEDTGAQVL LCSEIGSEGR NFQFASHMVM FDLPFNPDLL EQRIGRLDRI 600
GQAHDIQIHV PYLEKTAQSV LVRWYHEGLD AFEHTCPTGR TIYDSVYNDL INYLASPDQT EGFDDLIKNC REQHEALKAQ LEQGRDRLLE IHSNGGEKAQ 700
ALAESIEEQD DDTNLIAFAM NLFDIIGINQ DDRGDNMIVL TPSDHMLVPD FPGLSEDGIT ITFDREVALA REDAQFITWE HPLIRNGLDL ILSGDTGSST 800
ISLLKNKALP VGTLLVELIY VVEAQAPKQL QLNRFLPPTP VRMLLDKNGN NLAAQVEFET FNRQLNAVNR HTGSKLVNAV QQDVHAILQL GEAQIEKSAR 900
ALIDAARNEA DEKLSAELSR LEALRAVNPN IRDDELTAIE SNRQQVMESL DQAGWRLDAL RLIVVTHQ 968

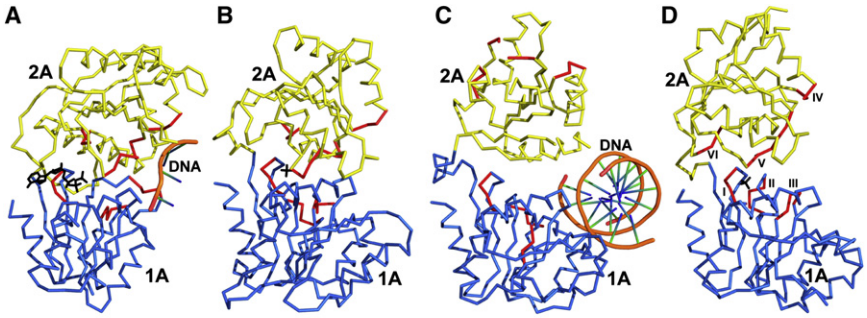

E

Domain	RecA-like Domain 1A		
Motif	I	II	III
Interaction [a]	MgATP	III, V, VI, Mg^{2+}	II, ATP, DNA
PcrA (3PJR) [b]	$_{31}$AGAGSGKT$_{38}$	$_{220}$IHIDEYQD$_{227}$	$_{250}$GDADQSIYPWR$_{260}$
ZfRad54 (1Z3I)	$_{177}$DEMGLGKT$_{184}$	$_{287}$VICDEGHR$_{294}$	$_{318}$SGTPIQEDLLY$_{328}$
SsRad54 (1Z63)	$_{469}$DDMGLGKT$_{476}$	$_{559}$IVIDEAQN$_{566}$	$_{590}$TGTPIEQKVDD$_{600}$
EcRapA	$_{177}$DEVGLGKT$_{184}$	$_{277}$LVVDEAHH$_{284}$	$_{313}$TATPEQLGMES$_{323}$

Domain	RecA-like Domain 2A		
Motif	IV	V	VI
Interaction [a]	DNA	II, DNA, ATP	II, ATP
PcrA (3PJR) [b]	$_{358}$YRTNAQSR$_{365}$	$_{563}$TLHAAKGLE$_{571}$	$_{606}$VGITRAEE$_{613}$
ZfRad54 (1Z3I)	$_{514}$SNYTQTLD$_{521}$	$_{567}$SKAGGCGLN$_{575}$	$_{596}$QAMARVWR$_{603}$
SsRad54 (1Z63)	$_{754}$TQFVDMGK$_{761}$	$_{807}$VKAGGFGIN$_{815}$	$_{839}$DRVYRIGQ$_{846}$
EcRapA	$_{510}$CAKAATAL$_{517}$	$_{563}$SEIGSEGRN$_{571}$	$_{595}$GRLDRIGQ$_{602}$

[a] According to Caruthers and McKay (2002). [b] PDB accession code.

Figure 3. RecA-like Architecture and the Six Conserved Functional Motifs

(A–D) The RacA-like architecture of DExx box helicase PcrA in complex with DNA and an ATP analog (PDB entry 2PJR), ZfRad54 in complex with a sulfate ion (PDB entry 1Z3I), SsRad54 in complex with dsDNA (PDB entry 1Z63), and *E. coli* RapA in complex with a sulfate ion are illustrated as Cα traces on the basis of the superposition of domain 1A. Domain 1A is shown in blue and 2A in yellow. Indicated in red are the six functional motifs, the sequences of which are shown in (E). The ATP and SO_4 are shown as stick models while DNA molecules as tubes.

(E) Structure-based sequence alignment for the six functional motifs in PcrA•ATP•DNA, ZfRad54•SO_4, SsRad54•DNA, and RapA•SO_4. Amino acid residues highlighted in red are also shown in red in (A—D). The functional motifs are labeled in (D) only. The roles (interactions) of the six functional motifs are predicted on the basis of helicase structures (Caruthers and McKay, 2002).

The Swi2/Snf2 proteins are ATP-dependent dsDNA translocases. In vitro, RapA binds both single-stranded and double-stranded polynucleotide molecules, but exhibits higher affinity for dsDNA (Sukhodolets and Jin, 1998). It has ATPase activity, which is stimulated upon its binding to RNAP (Sukhodolets and Jin, 2000). Therefore, RapA is likely an ATPase-dependent dsDNA translocase.

The arrangement of the four domains in the ATPase core of RapA (Figure 4A) is similar to that in the ZfRad54•SO_4 structure (PDB entry 1Z3I, Figure 4B), the "closed" conformation of Swi2/Snf2. Although the "open" form of Rad54 exhibits a 180° flip of the 2A/2B lobe (Figure 4C), the relative positioning of domain 2B with respect to 2A is unchanged. The arrangement of the four domains in the ATPase core of RapA supports the classification of the RapA group as a subfamily within the Swi2/Snf2 family, in spite of relatively lower sequence homology between RapA and the other 24 subfamilies (Flaus et al., 2006). Mfd, the bacterial transcription-repair coupling factor, is also a DNA translocase (Deaconescu et al., 2006). However, the ATPase core of Mfd (PDB entry 2EYQ) shows significant difference in the location and the orientation of domain 2B with respect to the 2A domain (Figure 4D).

Model of RapA in Complex with ATP and dsDNA

The superposition of domain 1A in PcrA•ATP•DNA (PDB entry 3PJR), SsRad54•DNA (PDB entry 1Z63), and RapA•SO_4 shows that the β-phosphate group in PcrA•ATP•DNA and the sulfate ion in RapA•SO_4 share the same binding site (not shown) and that the ssDNA in PcrA•ATP•DNA and one strand of the dsDNA in SsRad54•DNA share the same binding mode to the 1A domain (Figure 5A). These similarities suggest an ATP-binding site and a dsDNA-binding site on the ATPase core of RapA, leading to a model for the RapA•ATP•dsDNA complex (Figure 5B). The model suggests that the ATP may be bound to RapA in a similar manner as it is bound to PcrA (PDB entry 3PJR) and that the minor groove of dsDNA may interact with domains 1A, 2A, and 2B. Previously, it was shown that mutations in domain 2B of SsRad54 interfere with its catalytic activity (Dürr et al., 2005). Thus, both the structural and the biochemical data indicate the involvement of domain 2B in the translocation of Swi2/Snf2 proteins on dsDNA.

On the basis of remarkable structural and topological similarities of the RecA-like architectures found in Swi2/Snf2 enzymes and DExx box helicases, Dürr and coworkers proposed a unified mechanism for these proteins (2006). Despite many functional differences, members of both families bind the 3′-5′ strand at an equivalent site across the two RecA domains, indicating that the ATP-driven conformational changes of the RecA-like architecture transport DNA substrates via the 3′-5′ strand in analogous ways. Both the binding mode and the transporting direction of DNA in our RapA•ATP•dsDNA model are completely in agreement with the unified mechanism. The translocation direction of the ATPase core along the minor groove of dsDNA is opposite to the transporting direction of the DNA (Figure 5B).

Figure 2. Structure and Sequence Characteristics of RapA

(A) Stereoview shows the Cα trace of RapA. Every twentieth Cα position is labeled with the tenth Cα position between every two labels indicated with a sphere. The domain structure of the protein is color-coded as in Figure 1. The sulfate ion is shown as a stick model in black.

(B) Sequence of RapA with secondary structure elements indicated above. One N-terminal residue and six C-terminal residues were not observed. Underlined are the six functional motifs located in the RecA-like domains 1A and 2A of the ATPase core.

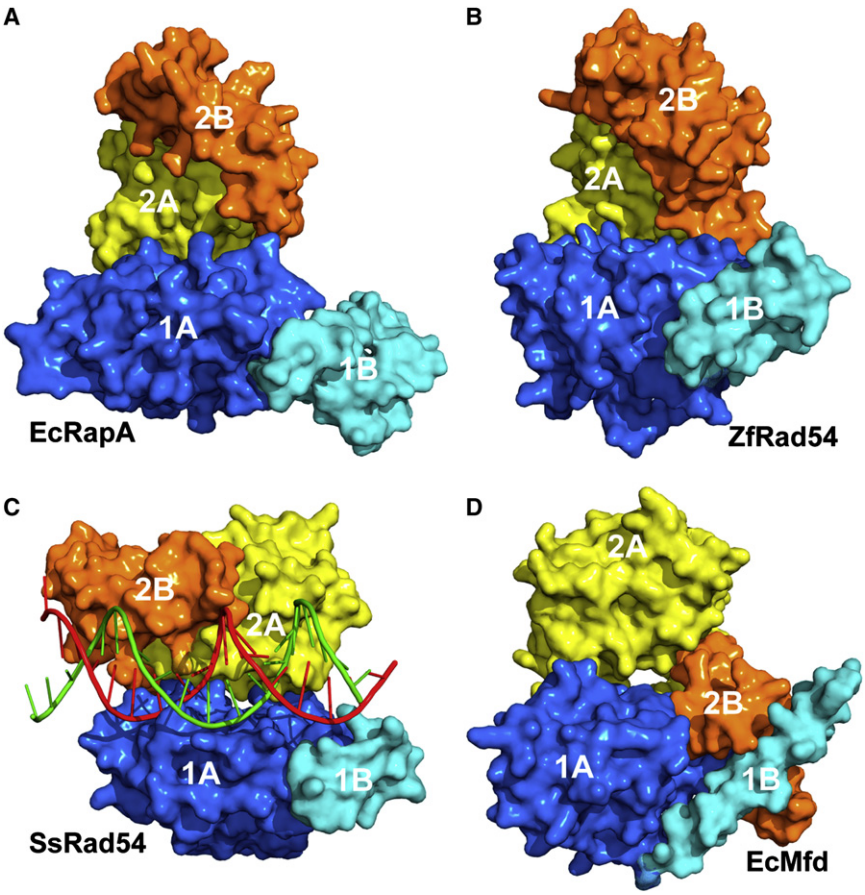

Figure 4. The ATPase Core of Swi2/Snf2 Proteins RapA and Rad54

(A–D) Domains 1A, 1B, 2A, and 2B in the ATPase core of *E. coli* RapA, ZfRad54 (PDB entry 1Z3I), SsRad54•DNA (PDB entry 1Z63), and *E. coli* Mfd (PDB entry 2EYQ) are illustrated as surface representation. The dsDNA in (C) is shown as a tube-and-stick model.

Kinetic Template-Switching Experiments

Thus far, the PTC is only operationally defined (Sukhodolets et al., 2001). It is known, however, that RapA binds to and forms a 1:1 complex with RNAP (Muzzin et al., 1998; Sukhodolets and Jin, 1998), that the ATPase activity of RapA is stimulated upon its binding to RNAP (Sukhodolets and Jin, 2000), and that RapA binds to DNA and RNA but exhibits higher affinity for dsDNA (McKinley and Sukhodolets, 2007; Muzzin et al., 1998; Sukhodolets and Jin, 1998). Therefore, the PTC can be an RNAP•DNA•RNA complex, an RNAP•DNA complex, or an RNAP•RNA complex. In this study, we tested whether RapA promotes the release of RNAP from the PTC using a kinetic template-switching assay.

As indicated in Figure 6, two DNA templates are used, each carrying a strong promoter, the *pTac* and the λP_L, respectively. Both templates also carry a weak promoter, *RNA1*, of which the activity is almost undetectable under the conditions used. Transcription terminators are positioned downstream of each promoter to give a distinguishing RNA product. RNAP is incubated with the first template containing the *pTac* and transcription is initiated by the addition of NTPs and allowed to finish (lane 1). If an equal molar amount of the second template containing the λP_L is added at the same time when the transcription of the *pTac* is initiated, small amounts of completed transcripts from both promoters are made, as would be expected if RNAP partitions between the two templates (lane 3). However, if the second template carrying the λP_L is added as little as 1 min after the transcription of the *pTac* is initiated, very little or no λP_L activity is observed (lanes 7, 9, and 11). In the latter case, almost all of the RNAP appears to initiate on the *pTac* only, which suggests that RNAP becomes sequestered in an arrested state with the first template and thus cannot be released for initiation at the λP_L introduced by the second template.

If RapA is added to these same transcription reactions (even number lanes, Figure 6), two differences are observed. First, the λP_L promoter from the second template can be transcribed very efficiently even when RapA is added 5 min after the initiation of the reaction. Second, the total transcription is increased for all promoters including the weak *RNA1* promoter. RapA appears to facilitate the release of RNAP from the PTC derived from the first template, which allows reinitiation of transcription at any available promoter thereby increasing the catalytic efficiency of RNAP. Because RNAP must dissociate from the PTC to initiate transcription *in trans* from the λP_L promoter located in the second template, the activity of RapA in the release of sequestered RNAP from the PTC is demonstrated.

Competition Between RapA and σ^{70} for Binding to RNAP In Vitro

We showed previously that RapA forms a complex with either the CORE or the HOLO (Sukhodolets and Jin, 1998, 2000); other studies have shown that the protein binds to the CORE but not to the HOLO (Muzzin et al., 1998). To further test whether RapA and σ^{70} compete for binding to the CORE, we performed in vitro competition experiment by monitoring the formation of the RapA•CORE and σ70•CORE complexes using gel filtration chromatography (Figure 7).

When the CORE and RapA are premixed in the presence of 0.3 M NaCl, a significant amount of RapA•CORE is detected and the complex is well separated from the free RapA (Figure 7A). However, when equal molar amounts of σ^{70} and RapA are added simultaneously to the CORE that is limiting, no RapA•CORE is detected; rather, only the σ70•CORE complex is formed (Figure 7B). Moreover, σ^{70} can readily replace RapA from preformed RapA•CORE, resulting in almost exclusive formation of the σ70•CORE complex (Figure 7C). These results are consistent with the notion that RapA and σ^{70} compete for binding to the CORE. In addition, the data demonstrate that the σ^{70}•CORE complex is more stable, in agreement with the previous reports

that the effective binding affinity of σ^{70} for RNAP is much higher than that of RapA (Gill et al., 1991; Muzzin et al., 1998; Sukhodolets and Jin, 2000). These results also provide an interpretation for the apparent association of RapA with HOLO we reported previously (Sukhodolets and Jin, 1998, 2000). If the HOLO fractions from the RNAP preparations are not saturated by σ^{70}, RapA will bind to the free CORE, resulting in an apparent RapA•HOLO complex, which is in fact a mixture of the σ^{70}•CORE and RapA•CORE complexes.

DISCUSSION

We have determined the first structure of *E. coli* RapA at 3.2-Å resolution, which is also the first full-length structure for the entire Swi2/Snf2 family of 1526 known members. The RapA molecule contains seven domains (Ntd, 1A, 1B, 2A, 2B, Spacer, and Ctd), among which the Spacer and Ctd exhibit novel protein folds (Figure 1). The Ntd contains two copies of a Tudor-like fold found in transcription factors NusG and Mfd (Deaconescu et al., 2006; Knowlton et al., 2003; Steiner et al., 2002). Domains 1A and 2A form the RecA-like architecture that is conserved among the DExx box helicases (Figure 3), while Domains 1A, 1B, 2A, and 2B form the ATPase core in which the arrangement of the four domains may be conserved among members of the Swi2/Snf2 family (Figure 4).

We have identified an ATP-binding site and a dsDNA-binding site on RapA, leading to a model of the RapA•ATP•dsDNA complex (Figure 5B), which is in agreement with the unified mechanism for Swi2/Snf2 enzymes and DExx box helicase proteins (Dürr et al., 2006). Our template-switching experiment shows that RNAP becomes sequestered in the PTC after one or few rounds of transcription and that RapA facilitates the release of immobilized RNAP from the PTC (Figure 6), thus demonstrating the role of RapA in mobilization of nucleic acid-protein complexes to facilitate transcription reinitiation. Our model and in vitro transcription data suggest that RapA may use its ATPase activity to remodel the PTC, leading to the release of sequestered RNAP from the PTC for transcription reinitiation. However, the mechanism underlying RapA remodeling of PTC remains to be elucidated. Although we demonstrated competition between RapA and σ^{70} in vitro (Figure 7), the mechanism underlying the competition is not understood at present. It is plausible that RapA and σ^{70} may share a common binding site or have partially overlapped binding sites on RNAP. Equally plausible, however, is that binding of σ^{70} to the CORE results in conformational changes of the CORE that preclude binding of RapA. The details of RapA-RNAP interactions remain to be further studied.

RapA, consistently copurified with RNAP (Muzzin et al., 1998; Sukhodolets and Jin, 1998), is as abundant as σ^{70} in the cell (Sukhodolets and Jin, 2000). Therefore, it is likely another general transcription factor. The structure of RapA provides a framework for further structural and biochemical investigations on, for example, the accurate RapA-binding site on RNAP, the exact composition of the PTC, how and where RNAP becomes sequestered in the PTC, the DNA translocase activity of RapA and its precise mechanism, and additional factors that may contribute to the destabilization of the PTC. Conceivably, such studies may also shed lights on how other Swi2/Snif2 proteins function in general.

EXPERIMENTAL PROCEDURES

Bacterial Strains and Plasmids Containing *rapA*

The bacterial media, genetic manipulations, and procedures used in this study have been described previously (Miller, 1972). The *rapA* clone (pDJ4374) used for overproduction of the recombinant RapA proteins were constructed as follows. The wt *rapA* gene from K12 MG1655 was amplified via polymerase chain reaction using the following primers: *rapA-10* F, 5′-CATGGATCC ATGCCT TT TACACTT GGTCAACGCT (BamHI site underlined) and *rapA-31*R, 5′-GCA AAGCTTACTGATGCGTTACAA (HindIII site underlined). The polymerase chain reaction products (~3 kb) were digested with BamHI and HindIII, and cloned into the expression vector pQE80L (QIAGEN), which was digested with the same restriction enzymes.

The *rap* (AA1-107) clone (pRapA107) used for overproduction of the RapA amino-terminus fragment (covering amino acid residual 1 to 107) was cloned similarly as the intact *rapA* clone described above, except that primer *rapA107HindIII* R (5′-AATTAAGCTTACACCAGTTTGCTATCAAGGA) was used in the place of *rapA-31*R.

The intact recombinant *rapA* clone and its derivatives were initially transformed into the XL Blue strain (Stratagene). These *rapA* clones all encoded few extra amino acid including 6 His residuals at the amino-terminus of the recombinant RapA proteins inherited from the expression vector. The sequences of these *rapA* clones were validated by DNA sequencing.

For overproduction of the recombinant RapA proteins that were incorporated with Selenomethionine (SeMet), the different *rapA* clones were transformed into the strain DJ791, which is auxotrophic for methionine in the K12 MG1655 background. DJ791 was constructed by phage P1 transduction to introduce a Tn10 (Kan) linked *met* mutation [met_{A28} *thi*::Tn10 (kan)] into strain DJ 624 which has a chromosomal $lacI^{Q}$ to ensure the repression of *rapA* in the absence of IPTG.

Overexpression of *rapA* and Purification of Recombinant RapA Proteins

Fresh cultures (1/100 dilution of overnight culture) were grown with shaking in the presence of ampicillin (100 μg/ml) at 37°C, either in LB or in a synthetic minimal SeMet medium (http://www.moleculardimensions.com) to synthesize SeMet-label RapA proteins. IPTG (final concentration 1mM) was added to the cultures when they reached OD_{600} ≈0.5 to induce expression of *rapA*. The induced cultures were then grown at 30°C for approximately 4 hr before cells were harvested by centrifugation. The resulting cell pastes were either stored at −80°C or used immediately for purification.

The recombinant RapA protein and its derivatives were purified essentially as described (Sukhodolets and Jin, 2000). The cell pellets were resuspended in 100 ml of extraction buffer (20 mM tris-HCl, 20 mM imidazole, 500 mM NaCl, and two tablets of protease inhibitor [pH 7.5]) and lysed using a homogenizer (APV). The lysed cell solution was centrifuged for 30 min at 15,000 × g. The supernatant was filtered before being loaded onto a nickel column (IMCA, GE HealthCare). A linear gradient was applied during the elution of the protein with buffer A (20 mM tris-HCl, 20 mM imidazole and 500 mM NaCl [pH 7.5]) and B (20 mM tris-HCl, 200 mM imidazole and 500 mM NaCl [pH 7.5]). Then, the fractionation was loaded onto de-salting column to exchange buffer from IMCA with sizing buffer (20 mM tri-HCl, 200 mM NaCl, 0.5 mM DTT and 1.0 mM EDTA [pH 7.5]). Finally, the protein solution was concentrated and loaded onto gel-filtration column Sephacryl S200 (GE HealthCare) and eluted with the sizing buffer. Mass spectrometry showed that 22 out of a total of 24 Met of RapA were converted into SeMet. The purified proteins were desalted, concentrated, and rapidly frozen in liquid N_2 and stored at −80°C.

Crystallization and X-ray Diffraction Data Collection

Crystallization screening was performed at 19 ± 1°C with a Hydra II Plus One robot (Matrix Liquid Handling Solutions, Thermo Fisher Scientific). Single crystals of the full length grew from the drops containing 0.3 μl protein solution (20 mM tris-HCl, 200 mM NaCl, 1.0 mM DTT and 1.0 mM EDTA [pH 7.5]) and 0.3 μl reservoir solution (1.6 M $AmSO_4$, 2.5% v/v 1,4-Dioxane, 10.% v/v ethyleneglycol and 0.1 M MES [pH 6.5]). Single crystals of the Ntd grew from the drops containing 0.2 μl protein solution (20 mM tris-HCl, 200 mM NaCl, 1.0 mM DTT, and 1.0 mM EDTA [pH7.5]) and 0.6 μl reservoir solution [200 mM $CA(OAc)_2$, 20% PEG8000 and 0.1 M MES (pH 6.5)].

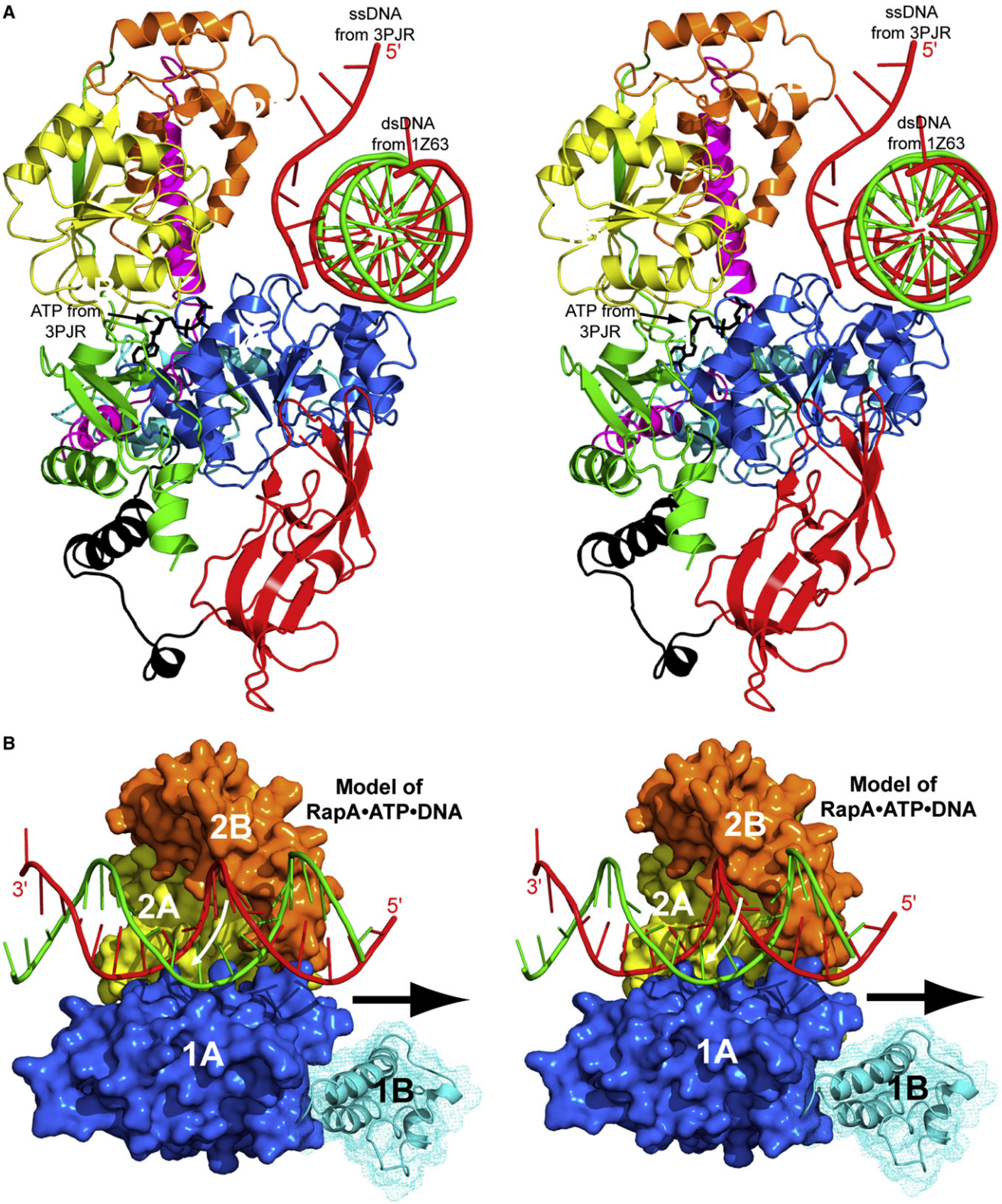

Figure 5. Hypothetical Model of the RapA•ATP•dsDNA Complex

(A) The ATPase core of RapA (ribbon diagram in the same color scheme defined in Figure 1) is shown with superimposed dsDNA (tube-and-stick model) from the SsRad54•DNA structure (PDB entry 1Z63), and the ATP (stick model) and a portion of ssDNA (tube-and-stick model) from the PcrA•ATP•DNA structure (PDB entry 3PJR). The SsRad54 and the PcrA are not shown for clarity.

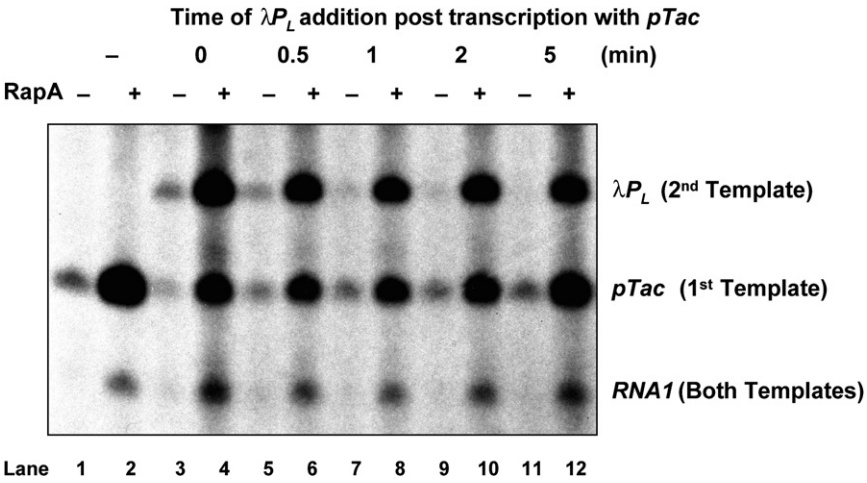

Figure 6. RapA Facilitates the Release of RNAP in an In Vitro DNA Template-Switch Transcription Assay

The reaction was started (as time 0) by the addition of NTPs into a preincubated complex of RNAP and a plasmid DNA containing *pTac* (the first template) either in the presence (+) or absence (–) of RapA; and at various times as indicated, an equal molar amount of another plasmid DNA containing λP_L (as a second template) was added, followed by 1-hr incubation for the reaction to complete. The transcripts for *pTac* and λP_L are indicated. The *RNAI* transcript from a relatively weak promoter present in both plasmids is also indicated.

X-ray diffraction data were collected at 100 K at the Advanced Photon Source, Argonne National Laboratory. Anomalous diffraction data for the full length were collected at the SBC-CAT beamline 19-ID equipped with an ADSC Quantum 315 CCD detector. Data for the Ntd were collected at the SER-CAT beamline 22-ID equipped with a MarResearch 300 CCD detector. Data processing was performed with the HKL program suite (Otwinowski and Minor, 1997). Inversion beam geometry was used to collect the SeMAD data for the full length, resulting in high completeness, high redundancy, and higher than average R_{merge} values. Statistics for the data are summarized in Table 1.

Structure Solution and Refinement

A total of 20 out of 22 incorporated Se atoms were found with SHELXD (Sheldrick et al., 1993) and refined with SHARP (de La Fortelle and Bricogne, 1997). The heavy atom phases were improved with DM and SOLOMON (Collaborative Computational Project Number 4, 1994). The resulting electron density was of higher than average quality for the resolution (Figure S2), which allowed an initial model containing 670 amino acid residues to be built. The crystal structure of SsRad54 (PDB entry 1Z63) assisted tracing the ATPase core although the sequence identity for the region between the two proteins was below 20%.

The initial structure was refined with the CNS (Brünger et al., 1998). A total of 2132 (4.6%) reflections were selected for cross validation (R_{free}). Bulk solvent correction was employed. During the refinement, the experimental phases were combined with model phases, which gradually generated electron density that enabled the inclusion of 184 more amino acid residues into the model, resulting in the Linker1-to-Ctd fragment (amino acid residues 108-962). Although insufficient to define the structure of the Ntd (amino acid residues 1-107), the electron density clearly outlined a domain structure that was tethered to the rest of RapA (Figure S1B). The Ntd structure was solved independently by the single wavelength anomalous diffraction (SAD) method at 2.15-Å resolution. The Se positions were identified with SOLVE (Terwilliger and Berendzen, 1999) and refined with SHARP (de La Fortelle and Bricogne, 1997). The heavy atom phases were improved with DM and SOLOMON (Collaborative Computational Project Number 4, 1994). Partial model was automatically built with RESOLVE (Terwilliger, 2002) and completed manually. The Ntd structure was then included into the full-length structure.

The crystal of the full-length RapA was twinned in space group $P4_3$, following the twin law h, -k, -l with a twin fraction of ½ . Nonetheless, the structure determination was performed in space group $P4_32_12$ until the refinement stuck at R = 0.34 and R_{free} = 0.38. The electron density was outstanding for the resolution and no additional structural features were revealed by phase combination. The refinement was then continued and finished in space group $P4_3$ with perfect merohedral twinning (Yeates, 1997).

Noncrystallographic symmetry restraints, treated separately for the Ntd and for the rest of the molecule, were enforced. The $2F_o–F_c$ and $F_o–F_c$ electron density maps were regularly calculated and examined. One sulfate ion was found for each RapA molecule, and no water molecule was identified. Only grouped B factors were refined. Upon completion, the entire structure was verified with the composite annealed omit map (Brünger et al., 1998). The final structure was assessed with PROCHECK (Laskowski et al., 1993). The statistics of the structure are summarized in Table 1. All graphics work was performed using the O program suite (Jones et al., 1991). Illustrations were prepared with PyMOL (DeLano, 2002).

Molecular Modeling

The RapA•ATP•dsDNA complex (Figure 5B) was modeled in three steps. First, on the basis of the superposition of domain 1A in PcrA•ATP•DNA (PDB entry 3PJR), SsRad54•DNA (PDB entry 1Z63) and RapA•SO_4, an ATP molecule was docked into the ATP-binding site and a putative DNA-binding site on RapA was located. The RMSD values for the superpositions are 2.65 Å for 127 pairs of Cα positions between PcrA and RapA, and 1.86 Å for 161 pairs of Cα positions between SsRad54 and RapA. Second, we removed the ssDNA and slightly adjusted the position of the dsDNA guided by the position of the ssDNA, and optimized the RapA•ATP•dsDNA model, during which the RapA, ATP, and dsDNA were treated as rigid bodies. Third, the energy of the model complex was minimized, which eliminated clashes between the protein and the ATP and DNA molecules. Both refinement steps were performed using the CNS program package (Brünger and Rice, 1997).

In Vitro Transcription Assays

The reactions were basically performed and analyzed as described previously (Sukhodolets et al., 2001). Briefly, the reaction was started by the addition of NTPs containing [α-^{32}P]UTP into a preincubated mix containing RNAP and plasmid (*pTac*) DNA with or without RapA at 37°C. At different time points as indicated in the legend of Figure 6, a second plasmid DNA (λP_L) was added into the reaction, followed by an additional 1 hr of incubation before the reaction was stopped. There are strong terminators after each of the three promoters (*pTac*, λP_L, and *RNA1*) in the plasmids used, resulting in transcripts with distinct sizes.

Competition of RapA and σ^{70} for Binding to CORE In Vitro

The CORE free of σ^{70} and active σ^{70} were purified as described (Zhi and Jin, 2003; Zhi et al., 2003). Complex formation of CORE with either σ^{70} or RapA

(B) The RapA•ATP•dsDNA model suggests a role of domain 2B in ATP-binding-associated advancement of dsDNA for Swi2/Snf2 proteins. In this view, the ATP molecule is not visible. The white arrow suggests the transporting direction of DNA; the black arrow suggests the translocation direction of the ATPase core along the minor groove of dsDNA. For clarity, only the ATPase core is shown instead of the full-length structure.

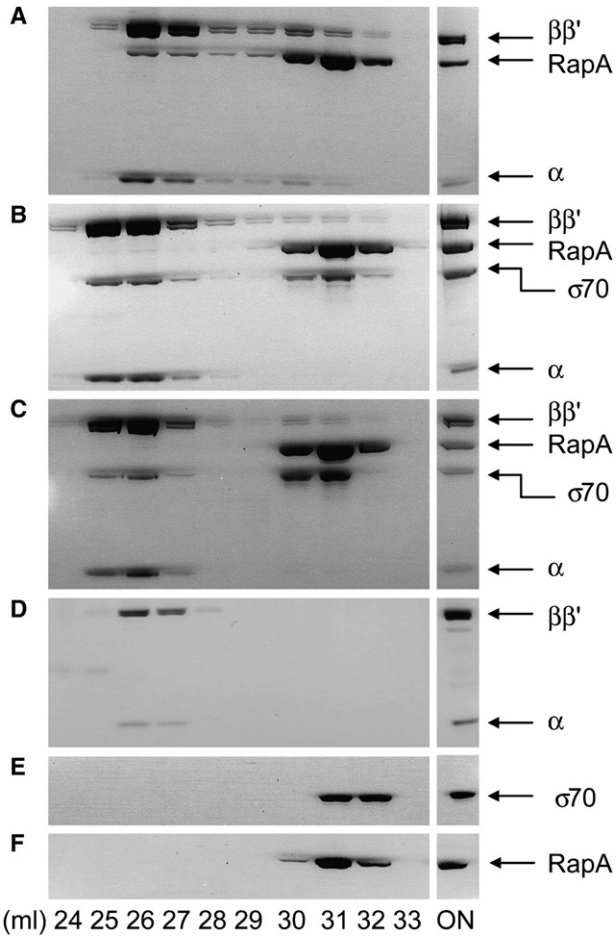

Figure 7. Gel Filtration Analyses: RapA and σ^{70} Compete for Binding to CORE In Vitro

The loaded protein mixture is indicated in the lane on the far right (ON). The positions for subunits of CORE, RapA, and σ^{70} are indicated. The concentration of each purified protein used in the representative set of experiments was 1 μM.

(A) RapA + CORE.

(B) (RapA + σ^{70}) + CORE. RapA and σ^{70} were premixed on ice followed by incubation with CORE at room temperature for 15 min.

(C) (RapA + CORE) + σ^{70}. RapA and CORE were premixed and incubated at room temperature for 15 min, followed by the addition of σ^{70} and incubation at room temperature for another 15 min.

(D–F) Controls of the experiment for CORE, σ^{70}, and RapA, respectively.

was studied essentially as described (Sukhodolets and Jin, 1998) with the following modifications. Two Superose-6 HR 10/30 columns (Amersham Biosciences), connected in tandem (total bed volume 48 ml), were used for better separation of the complexes from unbound protein. One μM of each purified protein was eluted either separately or premixed in 130 μl of TGED buffer (0.01M Tris [pH 7.9], 5% glycerol, 0.1 m M EDTA, and 0.1 mM DTT) containing 0.3 M NaCl. Unless otherwise stated, samples with two or more purified proteins were incubated at room temperature for 15 min before loading on the column that was pre-equilibrated with the above buffer. The column was run with the same buffer at a flow rate of 0.5 ml/min at 4°C, and the eluted fractions of 1.0 ml were collected using an AKTA system (Amersham Biosciences). Each fraction was concentrated using Microcon 30 concentrators (Amicon) at 4°C, and the samples were analyzed using a 4%–12% NuPAGE SDS gel (Invitrogen). The gels were stained by QuickBlue Stain (bostonbiologicals) and dried using Gel-Dry drying solution (Invitrogen).

ACCESSION NUMBERS

The coordinates and structure factors for the full-length SeMet-substituted RapA have been deposited with the Protein Data Bank (Rutgers, the State University of New Jersey) under the accession code 3DMQ.

SUPPLEMENTAL DATA

Supplemental Data include two figures and are available at http://www.structure.org/cgi/content/full/16/9/1417/DC1/.

ACKNOWLEDGMENTS

We thank Jack Simpson and Robert Fisher for help with mass spectrometry; Di Xia and Lothar Esser for help with cryoprotection; Michelle Andrykovitch for help with crystallization; Brian Austin and David Waugh for help with cloning; and Donald Court, Mikhail Kashlev, and Lucyna Lubkowski for discussion and review of the manuscript. X-ray diffraction and initial phasing were performed at the 19-ID beamline of SBC-CAT and the 22-ID beamline of SER-CAT, Advanced Photon Source, Argonne National Laboratory. This research was supported by the Intramural Research Program of the NIH, National Cancer Institute, Center for Cancer Research.

Received: May 3, 2008
Revised: June 11, 2008
Accepted: June 30, 2008
Published: September 9, 2008

REFERENCES

Ban, N., Nissen, P., Hansen, J., Moore, P.B., and Steitz, T.A. (2000). The complete atomic structure of the large ribosomal subunit at 2.4 Å resolution. Science *289*, 905–920.

Bork, P., and Koonin, E.V. (1993). An expanding family of helicases within the 'DEAD/H' superfamily. Nucleic Acids Res. *21*, 751–752.

Botuyan, M.V., Lee, J., Ward, I.M., Kim, J.E., Thompson, J.R., Chen, J., and Mer, G. (2006). Structural basis for the methylation state-specific recognition of histone H4–K20 by 53BP1 and Crb2 in DNA repair. Cell *127*, 1361–1373.

Brown, E., Malakar, S., and Krebs, J.E. (2007). How many remodelers does it take to make a brain? Diverse and cooperative roles of ATP-dependent chromatin-remodeling complexes in development. Biochem. Cell Biol. *85*, 444–462.

Brünger, A.T., and Rice, L.M. (1997). Crystallographic refinement by simulated annealing: methods and applications. Methods Enzymol. *277*, 243–269.

Brünger, A.T., Adams, P.D., Clore, G.M., DeLano, W.L., Gros, P., Grosse-Kunstleve, R.W., Jiang, J.S., Kuszewski, J., Nilges, M., Pannu, N.S., et al. (1998). Crystallography & NMR system: A new software suite for macromolecular structure determination. Acta Crystallogr. D *54*, 905–921.

Burgess, R.R., Erickson, B., Gentry, D.R., Gribskov, M., Hager, D., Lesley, S., Strickland, M., and Thompson, N. (1987). RNA Polymerase and the Regulation of Transcription (New York: Elsevier Science Publishing).

Caruthers, J.M., and McKay, D.B. (2002). Helicase structure and mechanism. Curr. Opin. Struct. Biol. *12*, 123–133.

CCP4 (Collaborative Computational Project Number 4). (1994). The CCP4 suite: programs for protein crystallography. Acta Crystallogr. D Biol. Cryallograph. *50*, 760–763.

de La Fortelle, E., and Bricogne, G. (1997). Maximum-likelihood heavy-atom parameter refinement for multiple isomorphous replacement and multiwavelength anomalous diffraction methods. Methods Enzymol. *276*, 472–494.

Deaconescu, A.M., Chambers, A.L., Smith, A.J., Nickels, B.E., Hochschild, A., Savery, N.J., and Darst, S.A. (2006). Structural basis for bacterial transcription-coupled DNA repair. Cell *124*, 507–520.

DeLano, W.L. (2002). The PyMOL Molecular Graphics System (San Carlos, CA: Delano Scientific).

Dirscherl, S.S., and Krebs, J.E. (2004). Functional diversity of ISWI complexes. Biochem. Cell Biol. *82*, 482–489.

Dürr, H., Korner, C., Muller, M., Hickmann, V., and Hopfner, K.P. (2005). X-ray structures of the *Sulfolobus solfataricus* SWI2/SNF2 ATPase core and its complex with DNA. Cell *121*, 363–373.

Dürr, H., Flaus, A., Owen-Hughes, T., and Hopfner, K.P. (2006). Snf2 family ATPases and DExx box helicases: differences and unifying concepts from high-resolution crystal structures. Nucleic Acids Res. *34*, 4160–4167.

Eisen, J.A., Sweder, K.S., and Hanawalt, P.C. (1995). Evolution of the SNF2 family of proteins: subfamilies with distinct sequences and functions. Nucleic Acids Res. *23*, 2715–2723.

Flaus, A., Martin, D.M., Barton, G.J., and Owen-Hughes, T. (2006). Identification of multiple distinct Snf2 subfamilies with conserved structural motifs. Nucleic Acids Res. *34*, 2887–2905.

Gill, S.C., Weitzel, S.E., and von Hippel, P.H. (1991). Escherichia coli sigma 70 and NusA proteins. I. Binding interactions with core RNA polymerase in solution and within the transcription complex. J. Mol. Biol. *220*, 307–324.

Holm, L., and Sander, C. (1996). Mapping the protein universe. Science *273*, 595–603.

Jones, T.A., Zou, J.Y., Cowan, S.W., and Kjeldgaard, M. (1991). Improved methods for building protein models in electron density maps and the location of errors in these models. Acta Crystallogr. A *47*, 110–119.

Knowlton, J.R., Bubunenko, M., Andrykovitch, M., Guo, W., Routzahn, K.M., Waugh, D.S., Court, D.L., and Ji, X. (2003). A spring-loaded state of NusG in its functional cycle is suggested by X-ray crystallography and supported by site-directed mutants. Biochemistry *42*, 2275–2281.

Kolsto, A.B., Bork, P., Kvaloy, K., Lindback, T., Gronstadt, A., Kristensen, T., and Sander, C. (1993). Prokaryotic members of a new family of putative helicases with similarity to transcription activator SNF2. J. Mol. Biol. *230*, 684–688.

Laskowski, R.A., MacArthur, M.W., Moss, D.S., and Thornton, J.M. (1993). PROCHECK: a program to check stereochemical quality of protein structures. J. Appl. Crystallogr. *26*, 283–291.

Laurent, B.C., Treich, I., and Carlson, M. (1993). The yeast SNF2/SWI2 protein has DNA-stimulated ATPase activity required for transcriptional activation. Genes Dev. *7*, 583–591.

Lewis, L.K., Jenkins, M.E., and Mount, D.W. (1992). Isolation of DNA damage-inducible promoters in Escherichia coli: regulation of polB (dinA), dinG, and dinH by LexA repressor. J. Bacteriol. *174*, 3377–3385.

McKinley, B.A., and Sukhodolets, M.V. (2007). Escherichia coli RNA polymerase-associated SWI/SNF protein RapA: evidence for RNA-directed binding and remodeling activity. Nucleic Acids Res. *35*, 7044–7060.

Miller, J.H. (1972). Experiments in Molecular Genetics (Cold Spring Harbor, NY: Cold Spring Harbor Laboratory).

Mohrmann, L., and Verrijzer, C.P. (2005). Composition and functional specificity of SWI2/SNF2 class chromatin remodeling complexes. Biochim. Biophys. Acta *1681*, 59–73.

Muzzin, O., Campbell, E.A., Xia, L., Severinova, E., Darst, S.A., and Severinov, K. (1998). Disruption of *Escherichia coli* hepA, an RNA polymerase-associated protein, causes UV sensitivity. J. Biol. Chem. *273*, 15157–15161.

Otwinowski, Z., and Minor, W. (1997). Processing of X-ray diffraction data collected in oscillation mode. Methods Enzymol. *276*, 307–326.

Pazin, M.J., and Kadonaga, J.T. (1997). SWI2/SNF2 and related proteins: ATP-driven motors that disrupt protein-DNA interactions? Cell *88*, 737–740.

Selenko, P., Sprangers, R., Stier, G., Buhler, D., Fischer, U., and Sattler, M. (2001). SMN tudor domain structure and its interaction with the Sm proteins. Nat. Struct. Biol. *8*, 27–31.

Sheldrick, G., Dauter, M., Wilson, K.S., Hope, H., and Sieker, L.C. (1993). The application of direct methods and Patterson interpretation to high-resolution native protein data. Acta Crystallogr. *D49*, 18–23.

Steiner, T., Kaiser, J.T., Marinkovic, S., Huber, R., and Wahl, M.C. (2002). Crystal structures of transcription factor NusG in light of its nucleic acid- and protein-binding activities. EMBO J. *21*, 4641–4653.

Sukhodolets, M.V., and Jin, D.J. (1998). RapA, a novel RNA polymerase-associated protein, is a bacterial homolog of SWI2/SNF2. J. Biol. Chem. *273*, 7018–7023.

Sukhodolets, M.V., and Jin, D.J. (2000). Interaction between RNA polymerase and RapA, a bacterial homolog of the SWI/SNF protein family. J. Biol. Chem. *275*, 22090–22097.

Sukhodolets, M.V., Cabrera, J.E., Zhi, H., and Jin, D.J. (2001). RapA, a bacterial homolog of SWI2/SNF2, stimulates RNA polymerase recycling in transcription. Genes Dev. *15*, 3330–3341.

Terwilliger, T.C. (2002). Automated structure solution, density modification and model building. Acta Crystallogr. D Biol. Crystallogr. *58*, 1937–1940.

Terwilliger, T.C., and Berendzen, J. (1999). Automated MAD and MIR structure solution. Acta Crystallogr. D Biol. Crystallogr. *55*, 849–861.

Thomä, N.H., Czyzewski, B.K., Alexeev, A.A., Mazin, A.V., Kowalczykowski, S.C., and Pavletich, N.P. (2005). Structure of the SWI2/SNF2 chromatin-remodeling domain of eukaryotic Rad54. Nat. Struct. Mol. Biol. *12*, 350–356.

Travers, A.A., and Burgess, R.R. (1969). Cyclic re-use of the RNA polymerase sigma factor. Nature *222*, 537–540.

Tsukiyama, T., and Wu, C. (1997). Chromatin remodeling and transcription. Curr. Opin. Genet. Dev. *7*, 182–191.

Velankar, S.S., Soultanas, P., Dillingham, M.S., Subramanya, H.S., and Wigley, D.B. (1999). Crystal structures of complexes of PcrA DNA helicase with a DNA substrate indicate an inchworm mechanism. Cell *97*, 75–84.

Wu, J., and Grunstein, M. (2000). 25 years after the nucleosome model: chromatin modifications. Trends Biochem. Sci. *25*, 619–623.

Yeates, T.O. (1997). Detecting and overcoming crystal twinning. Methods Enzymol. *276*, 344–358.

Zhi, H., and Jin, D.J. (2003). Purification of highly-active and soluble Escherichia coli sigma 70 polypeptide overproduced at low temperature. Methods Enzymol. *370*, 174–180.

Zhi, H., Yang, W., and Jin, D.J. (2003). Escherichia coli proteins eluted from mono Q chromatography, a final step during RNA polymerase purification procedure. Methods Enzymol. *370*, 291–300.